Cycloreversion

DOI: 10.1002/anie.200702474

The Thermal Retro[2+2+2]cycloaddition of Cyclohexane Activated by Triscyclobutenannelation: Concerted All-Disrotatory versus Stepwise Conrotatory Pathways to Fused [12]Annulenes**

Michael J. Eichberg, K. N. Houk, Jürg Lehmann, Philip W. Leonard, Anne Märker, Joseph E. Norton, Dorota Sawicka, K. Peter C. Vollhardt, Glenn D. Whitener, and Stefan Wolff*

The unknown C_{3v}-symmetric *all-cis* triscyclobutenocyclohexane **1**[1] is of fundamental interest as a key structure on which to probe the mechanism of [2+2+2]cycloreversions of cyclopropa- and cyclobuta-fused cyclohexanes ("tris-σ-homobenzenes").[1a,2] Thus, various examples of the cyclopropa-fused derivatives undergo facile $[\sigma^2_s+\sigma^2_s+\sigma^2_s]$ retrocyclization through aromatic transition states, whereas *all-cis* triscyclobutacyclohexane is deflected to a radical decomposition pathway,[3] which is the result of unfavorable through-bond interactions.[2c,d] In contrast, the double bonds in **1** should not only activate by introducing further strain,[4] but also enable additional orbital symmetry control in the form of stepwise conrotatory cyclobutene ring openings, conflicting stereochemically with a concerted all-disrotatory unraveling of the cyclohexane ring. While conrotatory motion is seemingly constrained in bicyclo[*n*.2.0]alkenes, leading to much speculation regarding the feasibility of forbidden disroratory pathways in such systems,[5] *cis*-bicyclo[4.2.0]oct-7-ene, the pertinent subunit of **1** (highlighted), chooses this option.[6] More generally, such cyclohexane cycloreversions constitute one strategy for gaining access to the interior of fullerenes.[7] In addition, triene **1** (and its derivatives) are of importance structurally, because of their potential central-ring planarity,[8] and synthetically, as new precursors to novel [12]annulene isomers[9] and as new 6π-electron ligands for catalysis.[10]

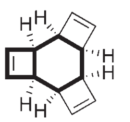

1

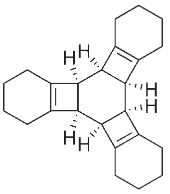

2

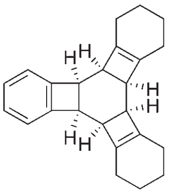

3

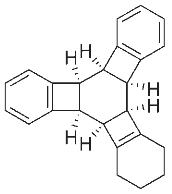

4

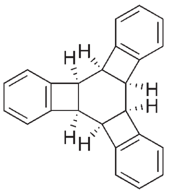

5

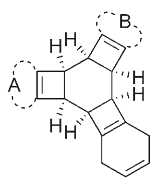

6a: A=B=–$CH_2CH=CHCH_2$–
6b: A=–$CH=CHCH=CH$–,
B=–$CH_2CH=CHCH_2$–
6c: A=B=–$CH=CHCH=CH$–

We report the synthesis, structure, and thermal rearrangement of the first example of structural motif **1**, namely the triply annelated hydrocarbon **2** and its congeners **3** and **4**, and compare their behavior to that of their common precursor, the trisbenzo analogue **5**,[11] for which all-disrotatory retro-[2+2+2]cycloaddition has been proposed.[11b] To assist in the interpretation of the results, DFT calculations were employed. These calculations suggested an unexpected switch-over in the mechanism of cyclohexane ring fissure along the series.

Birch reduction[12] of **5**[11b] could be controlled to give **6a**, either pure (93 %), or admixed with varying amounts (depending on the quantity of lithium used) of the mono-(**6b**) and bisbenzo relatives (**6c**), which were separated by column chromatography.[13] Selective dihydrogenation with Wilkinson's catalyst then furnished the targets **2**–**4**, respectively, in good yields. Inspection of the NMR spectroscopic data of the series **2**–**5** reveals the trends expected for progressive, peripheral aromatization. Noticeable are the fairly invariant chemical shifts of the central cyclohexane carbon atoms, namely $\delta = 43.3$, 42.3 (average), 41.5 (average), and 40.6 ppm, respectively, and the small shielding trend, reflecting that observed for the corresponding carbon atoms in cyclobutene ($\delta = 31.4$ ppm) and benzocyclobutene ($\delta = 29.5$ ppm). Because of their novelty, X-ray structural analyses

---

[*] Dr. M. J. Eichberg, Dr. J. Lehmann, Dr. P. W. Leonard, A. Märker, Prof. Dr. K. P. C. Vollhardt, Dr. G. D. Whitener, Dr. S. Wolff
Department of Chemistry, University of California at Berkeley
and
Chemical Sciences Division
Lawrence Berkeley National Laboratory
Berkeley, CA 94720-1460 (USA)
Fax: (+1) 510-643-5208
E-mail: kpcv@berkeley.edu
Homepage: http://chem.berkeley.edu/people/faculty/vollhardt/vollhardt.html

Prof. Dr. K. N. Houk, Dr. J. E. Norton, Dr. D. Sawicka
Department of Chemistry and Biochemistry
University of California, Los Angeles
Los Angeles, CA 90095 (USA)
Homepage: http://www.chem.ucla.edu/dept/Faculty/houk.html/

[**] This work was supported by the NSF (CHE 0451241 (K.P.C.V.), CHE-0548209 (K.N.H.), and predoctoral fellowships for M.J.E., P.W.L., J.E.N. (IGERT), and G.D.W.) We also thank the Swiss National Science Foundation (J.L.), Bayer-Miles (G.D.W.), and DFG (S.W.) for respective fellowships. Dr. Mary P. Watson provided excellent assistance with the Gepasi program.

Supporting information for this article is available on the WWW under http://www.angewandte.org or from the author.

were executed for **2**–**4** and **6a**.[13] The structure of **2** serves to illustrate the salient features of these compounds (Figure 1). The molecule was modeled with a crystallographic symmetry plane bisecting C7–C7′ and C9–C9′. The central cyclohexane ring is almost planar; C7-C8-C9 define a plane at an angle of 10.9° to the plane defined by C7-C7′-C9-C9′, leading to a shallow boat conformation. The cyclobutene rings are (nearly) planar and have interplanar angles of 54° (C1-C6-C7-C8) and 65° (C9-C9′-C10-C10′) relative to the central ring. The slightly distorted planar cyclohexane motif is maintained in **3**, **4**, and **6a**. This finding contrasts with the structure of **5**,[11b] with a planar core. There is strong bond alternation of the central ring in all structures, increasing very slightly in the order **2**, **6a** ≈ **4** ≈ **3**, and **5** (Σlong bonds−Σshort bonds = 0.187, 0.210, 0.220, 0.228, 0.264 Å, respectively). Overall, however, there is a remarkable structural similarity of substructure **1** in these hydrocarbons, except for the expected incrementally increased length of the double bonds as they become benzenoid (see Supporting Information). B3LYP/6-31G(d) optimized structures are in good agreement with these data (see Experimental Section and Supporting Information). For example, computed **2** (in threefold symmetry) contains an almost flat-chair cyclohexane center (average dihedral angles 6.6°), with a bond alternation of 0.195 Å, and the three cyclobutane moieties emanating at 56–57° angles.

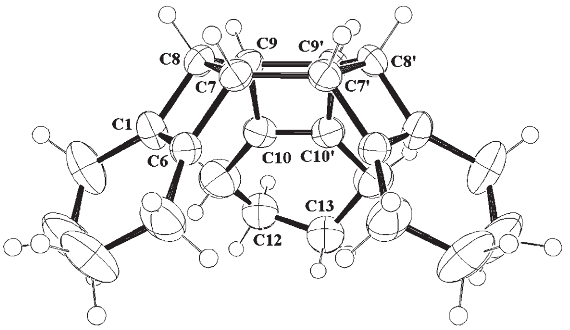

Figure 1. ORTEP representation of **2**; thermal ellipsoids are set at 50% probability. The disorder around C12 and C13 is not shown. Selected bond lengths [Å] and angles [°]: C1-C6 1.315(4), C6-C7 1.518(4), C7-C8 1.580(4), C1-C8 1.526(4), C8-C9 1.525(4), C9-C10 1.524(4), C7-C7′ 1.533(5), C10-C10′ 1.327(5); C6-C1-C8 95.1(2), C1-C6-C7 94.6(2), C6-C7-C8 85.42(19), C1-C8-C7 84.38(19), C7′-C7-C8 120.12(13), C7-C8-C9 119.1(2), C8-C9-C9′ 119.63 (14), C9′-C9-C10 84.66(14), C9-C10-C10′ 95.34(14), C6-C1-C8-C7 5.4(2), C7′-C7-C8-C9 −12.6(3).

Despite these structural similarities,[14] the thermal reorganization of **2**–**5** shows some marked differences (Scheme 1). Thus, along the series, **2** rearranges with the greatest facility and directly to cage compound **8a**.[15] With modestly increasing difficulty, monobenzo **3** forms **8b** regioselectively with concomitant steady-state presence of *all-cis* triene **7b** (monitored by ^{1}H NMR spectroscopy and kinetically modeled with the Gepasi 3.30 program).[16] Bisbenzo analogue **4** generates stable **7c**, which continues to **8c** regioselectively only at higher temperatures, and **5** stops at **7d**.[11] The relative rates of disappearance at 140°C along the series are 88:28:8:1; the measured activation parameters are compiled in Table 1. The structures of **8a**–**c**, the genesis of which will be discussed later, were confirmed by X-ray diffraction.[13] The stereochemistry of **7b** and **7c** followed from the characteristic ^{1}H NMR chemical shifts and coupling constants of the *cis*-alkene units.[11,13,17]

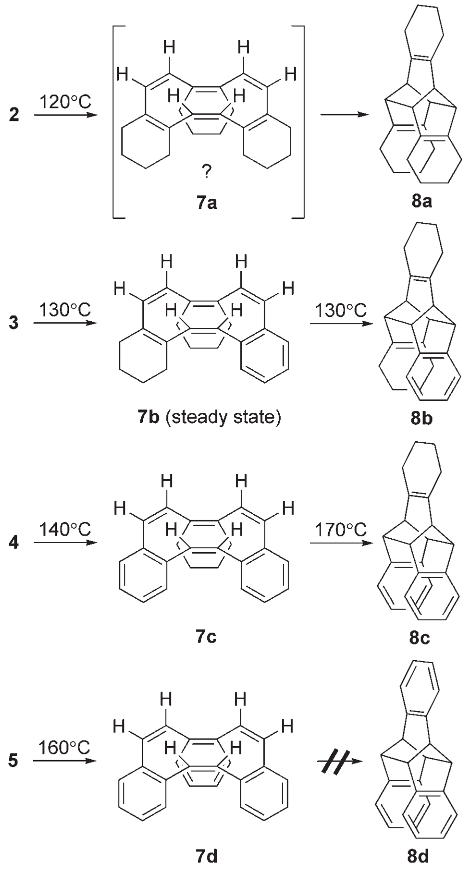

Scheme 1. Thermal isomerizations of **2**–**5**. The letters **a**–**d** in products **7**–**11** of this and subsequent Schemes refer to the respective triscyclohexeno, mono-, bis-, and trisbenzo derivatives.

A cursory appraisal of the results would suggest a common mechanism of the first step of these transformations, namely all-disrotatory cyclohexane retro-[2+2+2]cycloaddition to the corresponding *all-cis* [12]annulenes **7**, among which **7a** could be rendered unobservable by relatively fast further transformation to **8a**. However, calculations of this pathway revealed a trend, if small, opposite to that observed. In absolute terms, a $\Delta H^{\ddagger}$ value for **2** (34.6 kcal mol^{-1}) deviates from that measured beyond likely experimental[18a] and computational[18b,c] uncertainty (Table 1). On the other hand, probing the option of stepwise cyclobutene ring rupture uncovered a conrotatory, energetically close-lying manifold. It not only provided an acceptable $\Delta H^{\ddagger}$ value for **2** (opening of the first cyclobutene ring), but followed the opposite trend,[19] ending in a $\Delta H^{\ddagger}$ for **5** that is too large to be reconcilable with the experimental data (Table 1). In short, the theoretical data support the surprising notion that, while **5** unravels in a concerted all-disrotatory manner as originally reported,[11b] **2** chooses the stepwise conrotatory path (to furnish intermediate **9a**, Scheme 2). The corresponding values for **3** and **4** are too close to be of

Table 1: Experimental activation parameters for the thermal ring-opening reactions of compounds **2**–**5** and calculated B3LYP/6-31G(d) activation ($\Delta H^{\neq}$) and reaction (ΔH) enthalpies for concerted all-disrotatory versus stepwise conrotatory retrocyclization.[a]

Compound	$\Delta H^{\neq}_{exp}$ [kcal mol^{-1}]	$\Delta S^{\neq}_{exp}$ [e.u.]	$\Delta H^{\neq}_{calcd}$ (ΔH_{calcd}) concerted [kcal mol^{-1}]	$\Delta H^{\neq}_{calcd}$ (ΔH_{calcd}) stepwise [kcal mol^{-1}]
2	28.9(0.4)	−2.5(1.1)	34.6 (−25.6)	32.5 (−43.9)[b]
3	30.4(0.8)	−1.1(2.2)	33.9 (−29.7)	32.7 (−22.9)[b]
4	34.3(0.7)	5.9(1.7)	33.3 (−33.8)	33.4 (−42.0)[c]
5	34.1(1.0)	1.2(2.4)	32.6 (−38.0)	39.9 (−42.9)[d]

[a] For the structures of the transition states and the respective potential energy diagrams, see Supporting Information. [b] The first conrotatory cyclobutane ring opening is rate determining; the respective products are **9a** (Scheme 2) and its monobenzo analogue **9b**. [c] The first conrotatory cyclobutane ring opening is rate determining; the expected *all-trans* bis-*o*-xylylene isomer **9c** is not stable with B3LYP/6-31(d) and optimizes to 1,2-*trans*-5,6-*cis*-9,10-*trans*-bisbenzo[12]annulene, formed during the last ring opening by torsion of the double bonds and concomitant aromatization. [d] The third conrotatory cyclobutane ring opening is rate determining; the expected *all-trans* tris-*o*-xylylene isomer **9d** is not stable with B3LYP/6-31(d) and optimizes to *cis*,*trans*,*trans*-trisbenzo[12]annulene.

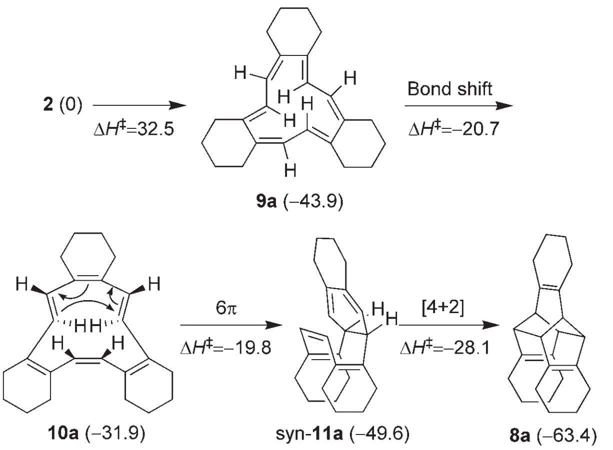

Scheme 2. Computed thermal isomerization of **2** to furnish **8a**. $\Delta H^{\neq}$ and (ΔH) values, calculated at the B3LYP/6-31G(d) level, are given relative to **2** (kcal mol^{-1}).

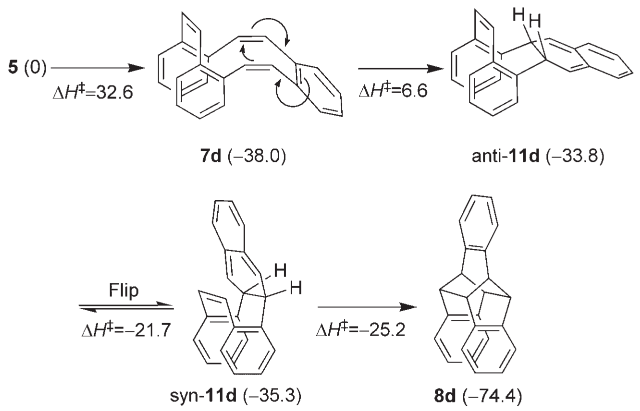

Scheme 3. Computed thermal isomerization of **5** to furnish **8d**. $\Delta H^{\neq}$ and (ΔH) values, calculated at the B3LYP/6-31G(d) level, are given relative to **5** (kcal mol^{-1}).

predictive value, but the exclusive experimental observation of intermediate trienes **7b** and **7c** indicates that these two systems mimic the behavior of **5**.

How and why are cage compounds **8a**–**c** formed, when **8d** is not, and what is the origin of the regioselectivity in the construction of **8b** and **c**? The answers give new insights into the effect of incremental benzofusion on the dynamic behavior of [12]annulene. Thus, as noted above, **2**, after all-conrotatory unstitching, generates **9a** (Scheme 2). This molecule has a geometry that is identical to that of Schröder's parent [12]annulene.[20] Experimentally,[20a] [12]annulene rearranges at −40 °C ($\Delta G^{\neq} = 17.4$ kcal mol^{-1}) to bicyclo-[6.4.0]dodecapentaene (the core of **11a**) via its *di-trans* isomer (as embedded in **10a**). Recent DFT calculations by Castro et al. have corroborated this pathway and pinpointed a Möbius aromatic transition state for bond shifting ($\Delta H^{\neq} = 18.0$ kcal mol^{-1}), followed by 6π-ring closure ($\Delta H^{\neq} = 17.8$ kcal mol^{-1}).[21] We find such a pathway also for **9a** proceeding to **10a** ($\Delta H^{\neq} = 23.2$ kcal mol^{-1})[22] and, subsequently ($\Delta H^{\neq} = 12.1$ kcal mol^{-1}), to the more stable (by 17.7 kcal mol^{-1}) syn-**11a**. Unlike the parent [12]annulene, which undergoes another electrocyclic closure to deliver a dimer of benzene and ultimately benzene itself,[20a] syn-**11a** finds it easier (with a barrier of 21.5 kcal mol^{-1}) to undergo intramolecular Diels–Alder addition to assemble **8a**. This scheme explains why **2** thermolyzes directly to **8a**.

At the other extreme lie **5** and its stable thermal product **7d**. In this connection, it is revealing that, while the *cis,cis,trans* and *trans,trans,trans* relatives of **7d** are similarly reluctant to rearrange, the *cis,trans,trans* isomer **10d** (the trisbenzo analogue of **10a**, Scheme 2) undergoes rearrangement to cage product **8d** at ambient temperatures.[11,17,23,24] The DFT data in Scheme 3 provide a rationale. Specifically, π-bond shift transition states on the path to **10d** could not be located for **7d**, presumably because of the required extensive loss of aromaticity of the benzene nuclei. Instead, a potential trajectory from **7d** to **11d** was found that featured direct 6π ring closure to anti-**11d**, followed by fast ring-flip,[25] and collapse to **8d**. However, the first step in this sequence requires *o*-xylylene formation and is energetically prohibitive ($\Delta H^{\neq} = 44.6$ kcal mol^{-1}) and endothermic by 4.2 kcal mol^{-1} (from **7d**), explaining our experimental findings. In contrast, the presence of one and two cyclohexene rings in **7c** and **7b**, respectively, changes the energetics of this step.[26] Thus, 6π electrocyclization of the diethenylcyclohexene portion of **7c** is calculated to require only 32.1 kcal mol^{-1} and to be exothermic to anti-**11c** (−16.7 kcal mol^{-1} from **7c**), followed by rapid ring-flip and regioselective creation of cage **8c** in which the cyclohexene ring is *ortho*-fused to the bridge of the bicyclo[2.2.2]octane core [Eq. (1) in Scheme 4]. Kinetic measurements of the rearrangement of **7c** result in $\Delta H^{\neq} = 30.5(1.4)$ kcal mol^{-1}, $\Delta S^{\neq} = -9.7(3.2)$ e.u., in excellent agree-

$$\mathbf{4}\ (0) \xrightarrow[\Delta H^{\ddagger}=33.3]{} \mathbf{7c}\ (-33.8) \xrightarrow[\Delta H^{\ddagger}=-1.7]{} \text{anti-}\mathbf{11c}\ (-50.5) \xrightarrow[\Delta H^{\ddagger}=-39.3]{} \text{syn-}\mathbf{11c}\ (-51.7) \xrightarrow[\Delta H^{\ddagger}=-33.3]{} \mathbf{8c}\ (-70.6) \qquad (1)$$

$$\mathbf{3}\ (0) \xrightarrow[\Delta H^{\ddagger}=33.9]{} \mathbf{7b}\ (-29.7) \xrightarrow[\Delta H^{\ddagger}=-2.4]{} \text{anti-}\mathbf{11b}\ (-48.2) \xrightarrow[\Delta H^{\ddagger}=-33.4]{} \text{syn-}\mathbf{11b}\ (-50.3) \xrightarrow[\Delta H^{\ddagger}=-31.4]{} \mathbf{8b}\ (-68.2) \qquad (2)$$

Scheme 4. Computed thermal isomerizations of **3** and **4** to furnish **8b** and **c**, respectively. ΔH^{+} and (ΔH) values, calculated at the B3LYP/6-31G(d) level, are given relative to starting materials (kcal mol^{-1}).

ment with theory. Similarly, **7b** undergoes this closure with $\Delta H^{+}_{\text{calcd}} = 27.3$ kcal mol^{-1}, in qualitative agreement with its observation as steady-state in the thermolysis of **3**, to give eventually only regioisomer **8b** [Eq. (2) in Scheme 4].

In summary, with hydrocarbon **2**, we have synthesized and structurally characterized the first example of the long-sought *all-cis* triscyclobutenocyclohexane framework, along with its hexadehydro (**6a**) and benzofused analogues (**3**–**5**). Unlike **3**–**5** and the tris-σ-homobenzenes, which undergo [$\sigma^2_s+\sigma^2_s+\sigma^2_s$] cycloreversion, **2** appears to prefer stepwise conrotatory cyclobutane ring openings as the mechanism of disassembly. The barriers for both processes are close-lying, in particular for the mixed systems **3** and **4**. While this finding is of fundamental importance, it may also shape synthetic strategies aimed at using core-substituted derivatives of **2** as the springboard for the generation of Möbius aromatic [12]annulenes.[27]

Experimental Section

2: colorless crystals; m.p. > 120 °C (decomp); ^{1}H NMR spectroscopy (300 MHz, $CDCl_3$): $\delta = 2.98$ (s, 6H), 2.04 (m, 6H), 1.80 (m, 6H), 1.63 (m, 12H) ppm; ^{13}C NMR spectroscopy (100 MHz, C_6D_6): $\delta = 144.9$, 43.3, 25.7, 23.6 ppm; IR (KBr): $\tilde{\nu} = 2928$, 2887, 2833, 2850, 1440, 1357, 1325, 1263, 1218, 1161, 1128, 904, 840, 804 cm^{-1}; MS (70 eV): m/z (%): 318 (25) [M^+], 199 (100),145 (15); high-resolution(HR) MS (electron impact, EI): calcd for $C_{24}H_{30}$: 318.2348; found: 318.2347. Elemental analysis (%) calcd for $C_{24}H_{30}$: C 90.51, H 9.49; found: C 90.55, H 9.36. **8a**: colorless crystals; m.p. 161–162 °C; ^{1}H NMR spectroscopy (300 MHz, $CDCl_3$): $\delta = 2.97$ (quin, $J = 1.7$ Hz, 2H), 2.08 (m, 4H), 1.98 (m, 8H), 1.75 (t, $J = 1.7$ Hz, 4H), 1.70–1.55 (m, 12H) ppm; ^{13}C NMR spectroscopy (100 MHz, C_6D_6): $\delta = 144.9$, 136.3, 62.7, 50.1, 27.7, 26.8, 23.92, 23.90 ppm; IR (KBr): $\tilde{\nu} = 2925$, 2900, 2830, 1455, 1440, 1265, 1200, 1155, 1130, 867 cm^{-1}; MS (70 eV): m/z (%): 318 (66) [M^+], 275 (12), 261 (10), 223 (21), 199 (100); HRMS (EI): calcd for $C_{24}H_{30}$: 318.2348; found: 318.2342. Elemental analysis (%) calcd for $C_{24}H_{30}$: C 90.51, H 9.49; found: C 90.15, H 9.32.

Computational procedure: Conformational searches were performed using the MM2* force-field implemented in MacroModel Version 7.1 to identify lowest energy intermediates. These species were optimized at the B3LYP/6-31G(d) level of theory as implemented in Gaussian 03.[28] Critical points corresponding to reactants, products, intermediates, and transition structures were fully optimized. Vibrational frequencies were computed to confirm stationary points and to verify that transition structures corresponded to appropriate reaction coordinates. Unless otherwise noted, all energies are reported as thermally corrected enthalpies at 298 K.

Received: June 7, 2007

Keywords: ab initio calculations · cage compounds · electrocyclic reactions · isomerization · strained molecules

---

[1] a) For a seemingly abortive effort, see: C. Rücker, H. Müller-Bötticher, W.-D. Braschwitz, H. Prinzbach, U. Reifenstahl, H. Irngartinger, *Liebigs Ann./Recueil* **1997**, 967; b) the *trans*-perfluoroderivative has been claimed: W. R. Hertler, *J. Fluorine Chem.* **1975**, *6*, 171.

[2] a) For a review, see: A. de Meijere, S. I. Kozhushkov, H. Schill, *Chem. Rev.* **2006**, *106*, 4926; see also: b) A. de Meijere, C.-H. Lee, B. Bengtson, E. Pohl, S. I. Kozhushkov, P. R. Schreiner, R. Boese, T. Haumann, *Chem. Eur. J.* **2003**, *9*, 5481; c) D. Sawicka, K. N. Houk, *J. Mol. Model.* **2000**, *6*, 158; d) D. Sawicka, K. N. Houk, *J. Chem. Soc. Perkin Trans. 2* **1999**, 2349.

[3] M. Maas, M. Lutterbeck, D. Hunkler, H. Prinzbach, *Tetrahedron Lett.* **1983**, *24*, 2143.

[4] A. Fattahi, L. Lis, Z. Tian, S. R. Kass, *Angew. Chem.* **2006**, *118*, 5106; *Angew. Chem. Int. Ed.* **2006**, *45*, 4984.

[5] a) J. J. Gajewski, *Hydrocarbon Thermal Isomerizations*, Academic, New York, **1981**; for a more recent discussion, see:b) P. S. Lee, S. Sakai, P. Hörstermann, W. R. Roth, E. A. Kallel, K. N. Houk, *J. Am. Chem. Soc.* **2003**, *125*, 5839, and references therein.

[6] a) C. Silva López, O. N. Faza, Á. R. de Lera, *Org. Lett.* **2006**, *8*, 2055, and references therein; b) the power of orbital-symmetry control is evident even in the aromatization of Dewar benzene:R. W. A. Havenith, L. W. Jenneskens, J. H. van Lenthe, *J. Mol. Struct. (Theochem)* **1999**, *492*, 217.

[7] a) S.-C. Chuang, F. R. Clemente, S. I. Khan, K. N. Houk, Y. Rubin, *Org. Lett.* **2006**, *8*, 4525, and references therein; b) Y. Rubin, *Top. Curr. Chem.* **1999**, *199*, 67.

[8] a) H. Dodziuk, M. Ostrowski, *Eur. J. Org. Chem.* **2006**, 5231, and references therein; b) H. Dodziuk, *Top. Stereochem.* **1994**, *21*, 351.

[9] For a review, see: E. L. Spitler, C. A. Johnson II, M. M. Haley, *Chem. Rev.* **2006**, *106*, 5344.

[10] a) See, for example: A. Pla-Quintana, A. Torrent, A. Dachs, A. Roglans, R. Pleixats, M. Moreno-Mañas, T. Parella, J. Benet-Buchholz, *Organometallics* **2006**, *25*, 5612; b) review: C. Moberg, *Angew. Chem.* **1998**, *110*, 260; *Angew. Chem. Int. Ed.* **1998**, *37*, 248.

[11] a) Y. Kuwatani, T. Yoshida, A. Kusaka, M. Oda, K. Hara, M. Yoshida, H. Matsuyama, M. Iyoda, *Tetrahedron* **2001**, *57*, 3567; b) D. L. Mohler, K. P. C. Vollhardt, S. Wolff, *Angew. Chem.* **1990**, *102*, 1200; *Angew. Chem. Int. Ed. Engl.* **1990**, *29*, 1151.

[12] See also: R. Eckrich, D. Kuck, *Synlett* **1993**, 344.

[13] All new compounds gave satisfactory analytical and spectral data (see Experimental Section and Supporting Information). Hydrocarbons **2**–**4**, **6a**, and **8a**–**c** were subjected to X-ray crystallographic analysis. **2**: $C_{24}H_{30}$, crystal size $0.34 \times 0.21 \times 0.12$ mm^3, space group *Pnma*, scan range $3.0 < 2\theta < 50.9°$, $T = 158(2)$ K, $a = 9.7048(19)$, $b = 16.116(3)$, $c = 11.813(2)$ Å, $\alpha = 90.00$, $\beta = 90.00$, $\gamma = 90.00°$, $V = 1847.5(6)$ Å^3, $Z = 4$, $\rho_{\text{calcd}} = 1.145$ g cm^{-3}, $\mu(\text{Mo}_{K\alpha}) = 0.64$ cm^{-1}, 1666 unique reflections, of which 1044 were taken as observed [$I > 2\sigma(I)$], $R = 0.0688$, $R_w = 0.2024$. **3**: $C_{24}H_{26}$, crystal size $0.27 \times 0.17 \times 0.15$ mm^3, space group *Pnma*, scan range $3.0 < 2\theta < 51.1°$, $T = 151(2)$ K, $a = 9.6383(19)$, $b = 16.060(3)$, $c = 11.372(2)$ Å, $\alpha = 90.00$, $\beta = 90.00$, $\gamma = 90.00°$, $V = 1760.3(6)$ Å^3, $Z = 4$, $\rho_{\text{calcd}} = 1.187$ g cm^{-3}, $\mu(\text{Mo}_{K\alpha}) = 0.66$ cm^{-1}, 1589 unique reflections, of which 920 were taken as

observed $[I > 2\sigma(I)]$, $R = 0.0692$, $R_w = 0.2170$. **4**: $C_{24}H_{22}$, crystal size $0.27 \times 0.21 \times 0.09$ mm^3, space group *Pbca*, scan range $3.0 < 2\theta < 51.4°$, $T = 169(2)$ K, $a = 11.144(2)$, $b = 9.4561(19)$, $c = 31.587(6)$ Å, $\alpha = 90.00$, $\beta = 90.00$, $\gamma = 90.00°$, $V = 3328.8(11)$ Å^3, $Z = 8$, $\rho_{calcd} = 1.239$ g cm^{-3}, $\mu(Mo_{K\alpha}) = 0.70$ cm^{-1}, 2913 unique reflections, of which 1483 were taken as observed $[I > 2\sigma(I)]$, $R = 0.0510$, $R_w = 0.1366$. **6a**: $C_{24}H_{24}$, crystal size $0.26 \times 0.25 \times 0.02$ mm^3, space group *Pnma*, scan range $3.0 < 2\theta < 76.2°$, $T = 183(2)$ K, $a = 9.3537(13)$, $b = 16.308(2)$, $c = 11.1624(15)$ Å, $\alpha = 90.00$, $\beta = 90.00$, $\gamma = 90.00°$, $V = 1702.7(4)$ Å^3, $Z = 4$, $\rho_{calcd} = 1.219$ g cm^{-3}, $\mu(Mo_{K\alpha}) = 0.68$ cm^{-1}, 1617 unique reflections, of which 848 were taken as observed $[I > 2\sigma(I)]$, $R = 0.0460$, $R_w = 0.0819$. **8a**: $C_{24}H_{30}$, crystal size $0.38 \times 0.30 \times 0.30$ mm^3, space group *C*2/*c*, scan range $3.0 < 2\theta < 50.9°$, $T = 154(2)$ K, $a = 15.3310(15)$, $b = 12.0822(12)$, $c = 10.2586(10)$ Å, $\alpha = 90.00$, $\beta = 113.147(2)$, $\gamma = 90.00°$, $V = 1747.3(3)$ Å^3, $Z = 4$, $\rho_{calcd} = 1.211$ g cm^{-3}, $\mu(Mo_{K\alpha}) = 0.67$ cm^{-1}, 1484 unique reflections, of which 1224 were taken as observed $[I > 2\sigma(I)]$, $R = 0.0372$, $R_w = 0.0919$. **8b**: $C_{24}H_{26}$, crystal size $0.25 \times 0.18 \times 0.13$ mm^3, space group $P2_1/c$, scan range $3.0 < 2\theta < 50.9°$, $T = 183(2)$ K, $a = 11.076(3)$, $b = 9.683(3)$, $c = 16.217(4)$ Å, $\alpha = 90.00$, $\beta = 104.689(4)$, $\gamma = 90.00°$, $V = 1682.4(8)$ Å^3, $Z = 4$, $\rho_{calcd} = 1.234$ g cm^{-3}, $\mu(Mo_{K\alpha}) = 0.69$ cm^{-1}, 2844 unique reflections, of which 1411 were taken as observed $[I > 2\sigma(I)]$, $R = 0.0676$, $R_w = 0.1629$. **8c**: $C_{24}H_{22}$, crystal size $0.28 \times 0.19 \times 0.12$ mm^3, space group $P2_1/c$, scan range $3.0 < 2\theta < 51.2°$, $T = 169(2)$ K, $a = 10.8016(11)$, $b = 9.7448(10)$, $c = 16.0831(17)$ Å, $\alpha = 90.00$, $\beta = 104.760(2)$, $\gamma = 90.00°$, $V = 1637.0(3)$ Å^3, $Z = 4$, $\rho_{calcd} = 1.259$ g cm^{-3}, $\mu(Mo_{K\alpha}) = 0.71$ cm^{-1}, 2771 unique reflections, of which 1876 were taken as observed $[I > 2\sigma(I)]$, $R = 0.0428$, $R_w = 0.1108$. CCDC 648165–CCDC 648171 contain the supplementary crystallographic data for this paper. These data can be obtained free of charge from The Cambridge Crystallographic Data Centre via www.ccdc.cam.ac.uk/data_request/cif.

[14] A series of isodesmic and homodesmotic reactions indicates that the relative strain energy increases slightly in the order **2**→**5**. For example, the homodesmotic equation **5** + cyclohexene→**4** + benzene and its analogues yielding **3** and **2**, starting from **4** and **3**, respectively, gives strain = 0, 2.0, 4.7, and 8.5 kcal mol^{-1} along the series (see Supporting Information).

[15] The triple Birch-reduction product **6a** behaves as **2** and converts quantitatively into the hexadehydro analogue of **8a** at 130 °C (see Supporting Information).

[16] P. Mendes, *Trends Biochem. Sci.* **1997**, *22*, 361.

[17] For model systems, see: H. A. Staab, F. Graf, K. Doerner, A. Nissen, *Chem. Ber.* **1971**, *104*, 1159.

[18] a) We originally reported $\Delta H^{\neq} = 29.4(4.7)$ kcal mol^{-1}, $\Delta S^{\neq} = -12.7(11.3)$ for the thermolysis of **5** (see ref. [11b]), supplanted by Iyoda and coworkers (see ref. [11a]), $\Delta H^{\neq} = 32.7(0.9)$ kcal mol^{-1}, $\Delta S^{\neq} = 1.8(2.0)$, within error bars of our current data; for an appraisal of the performance of various methods in the estimation of activation barriers and structures, see, for example b) D. H. Ess, K. N. Houk, *J. Phys. Chem. A* **2005**, *109*, 9542, and references therein; c) R. A. Pascal, Jr., *J. Phys. Chem. A* **2001**, *105*, 9040.

[19] a) The observed trends in activation barriers follow the relative energies of the products formed after the rate-determining transition states (see Supporting Information); b) At the suggestion of a referee, we have calculated the data in Table 1 also at the B3PW91/6-31Gc) level of theory, revealing the same trends and "crossover" in mechanism.

[20] a) J. F. M. Oth, H. Röttele, G. Schröder, *Tetrahedron Lett.* **1970**, *11*, 61; b) C. Castro, W. L. Karney, C. M. H. Vu, S. E. Burkhardt, M. A. Valencia, *J. Org. Chem.* **2005**, *70*, 3602.

[21] C. Castro, W. L. Karney, M. A. Valencia, C. M. H. Vu, R. P. Pemberton, *J. Am. Chem. Soc.* **2005**, *127*, 9704.

[22] This isomer emerges initially as the unsymmetrical rotamer. Fast *trans*-double-bond rotation in [12]annulene is well established, see refs. [20, 21].

[23] This transformation was proposed to proceed by direct [2+2+2] (homo-Diels–Alder) cycloaddition. However, transition states for such one-step connections between **10** and **8** could not be located computationally. Instead, 6π closure ($\Delta H^{\neq} = 24.1$ kcal mol^{-1} from **10d**) was found to give syn-**11d** ($\Delta H^{\neq} = 3.5$ kcal mol^{-1}), which continues on to **8d** (Scheme 3).

[24] a) T. Yoshida, Y. Kuwatani, K. Hara, M. Yoshida, H. Matsuyama, M. Iyoda, S. Nagase, *Tetrahedron Lett.* **2001**, *42*, 53; b) M. D. Banciu, I. Simion, A. Banciu, A. Petride, C. Drăghici, *Rev. Roum. Chim.* **1991**, *36*, 1101; c) M. W. Tausch, M. Elian, A. Bucur, E. Cioranescu, *Chem. Ber.* **1977**, *110*, 1744; d) H. Irngartinger, *Chem. Ber.* **1975**, *108*, 1017.

[25] For experimental data on the conformational mobility of related bisbenzocyclooctatrienes, see: a) H. Meier, H. Gugel, M. Barth, U. Plücken, *Z. Naturforsch. B* **1980**, *35*, 477; b) T. S. Cantell, J. V. Silverton, *J. Org. Chem.* **1979**, *44*, 4477.

[26] For the 6π-ring closures of 1,2-diethenylcyclohexenes, see a) E. N. Marvell, C. Hilton, M. Cleary, *J. Org. Chem.* **1983**, *48*, 4272; b) E. N. Marvell, G. Caple, C. Delphey, J. Platt, N. Polston, J. Tashiro, *Tetrahedron* **1973**, *29*, 3797.

[27] C. Castro, C. M. Isborn, W. L. Karney, M. Mauksch, P. v. R. Schleyer, *Org. Lett.* **2002**, *4*, 3431.

[28] Gaussian 03 (Revision C.02): M. J. Frisch et al., see Supporting Information.